

# Modeling neutrophil migration in dynamic chemoattractant gradients: assessing the role of exosomes during signal relay

Alex C. Szatmary<sup>a,†</sup>, Ralph Nossal<sup>a</sup>, Carole A. Parent<sup>b,‡,\*</sup>, and Ritankar Majumdar<sup>b,‡,\*</sup>

<sup>a</sup>Division of Basic and Translational Biophysics, National Institute of Child Health and Human Development, Rockville, MD 20847; <sup>b</sup>Laboratory of Cellular and Molecular Biology, Center for Cancer Research, National Cancer Institute, National Institutes of Health, Bethesda, MD 20892

**ABSTRACT** Migrating cells often exhibit signal relay, a process in which cells migrating in response to a chemotactic gradient release a secondary chemoattractant to enhance directional migration. In neutrophils, signal relay toward the primary chemoattractant N-formylmethionyl-leucyl-phenylalanine (fMLP) is mediated by leukotriene B<sub>4</sub> (LTB<sub>4</sub>). Recent evidence suggests that the release of LTB<sub>4</sub> from cells occurs through packaging in exosomes. Here we present a mathematical model of neutrophil signal relay that focuses on LTB<sub>4</sub> and its exosome-mediated secretion. We describe neutrophil chemotaxis in response to a combination of a defined gradient of fMLP and an evolving gradient of LTB<sub>4</sub>, generated by cells in response to fMLP. Our model enables us to determine the gradient of LTB<sub>4</sub> arising either through directed secretion from cells or through time-varying release from exosomes. We predict that the secondary release of LTB<sub>4</sub> increases recruitment range and show that the exosomes provide a time delay mechanism that regulates the development of LTB<sub>4</sub> gradients. Additionally, we show that under decaying primary gradients, secondary gradients are more stable when secreted through exosomes as compared with direct secretion. Our chemotactic model, calibrated from observed responses of cells to gradients, thereby provides insight into chemotactic signal relay in neutrophils during inflammation.

**Monitoring Editor**  
Alex Mogilner  
New York University

Received: May 19, 2017  
Revised: Sep 15, 2017  
Accepted: Sep 19, 2017

## INTRODUCTION

Many biological processes such as wound healing, angiogenesis, and immune responses require cells to migrate directionally when subjected to external chemical gradients (Jin *et al.*, 2008). Many of these chemotactic events feature signal relay, a process by which

cells, on exposure to a primary end-point chemoattractant, release a secondary chemoattractant to increase the robustness of the initial chemotactic response by mediating intercellular communication (Majumdar *et al.*, 2014). Signal relay has been well studied in the social amoeba *Dictyostelium discoideum*, where cells chemotaxing toward cAMP regulate collective motility by further releasing cAMP (Garcia and Parent, 2008). In addition, CCL3 and CXCL18 have been shown to be released by monocytes and dendritic cells as secondary chemoattractants in response to the primary chemoattractant serum amyloid A (Gouwy *et al.*, 2015); T-cells secrete the XCR1 ligand XCL1 (Kelner *et al.*, 1994), which has been shown to attract dendritic cells and regulate T-cell effector function *in vitro* (Dorner *et al.*, 2009).

Neutrophils use signal relay to coordinate their motion through the release of the lipid eicosanoid leukotriene B<sub>4</sub> (LTB<sub>4</sub>) (Afonso *et al.*, 2012). Small molecules such as complement factors, released during tissue injury, or formyl peptides such as N-formylmethionyl-leucyl-phenylalanine (fMLP), released during bacterial infection, constitute primary chemotactic mediators of neutrophil chemotaxis. Ligand binding to cell surface receptors initiates leukotriene

This article was published online ahead of print in MBoc in Press (<http://www.molbiolcell.org/cgi/doi/10.1091/mbc.E17-05-0298>) on September 27, 2017.

Present addresses: <sup>†</sup>Department of Engineering, King's College, PA 18711; <sup>‡</sup>Department of Pharmacology, Michigan Medicine, Life Sciences Institute, University of Michigan, Ann Arbor, MI 48109.

\*Address correspondence to: Ritankar Majumdar ([ritankar@umich.edu](mailto:ritankar@umich.edu)) and Carole A. Parent ([parentc@umich.edu](mailto:parentc@umich.edu)).

Abbreviations used: BLT, leukotriene B<sub>4</sub> receptor; cAMP, cyclic adenosine monophosphate; DFRO, difference in fractional receptor occupancy; fMLP, N-formylmethionyl-leucyl-phenylalanine; FPR, formyl peptide receptor; LTB<sub>4</sub>, leukotriene B<sub>4</sub>.

© 2017 Szatmary *et al.* This article is distributed by The American Society for Cell Biology under license from the author(s). Two months after publication it is available to the public under an Attribution–Noncommercial–Share Alike 3.0 Unported Creative Commons License (<http://creativecommons.org/licenses/by-nc-sa/3.0>).

“ASCB®,” “The American Society for Cell Biology®,” and “Molecular Biology of the Cell®” are registered trademarks of The American Society for Cell Biology.



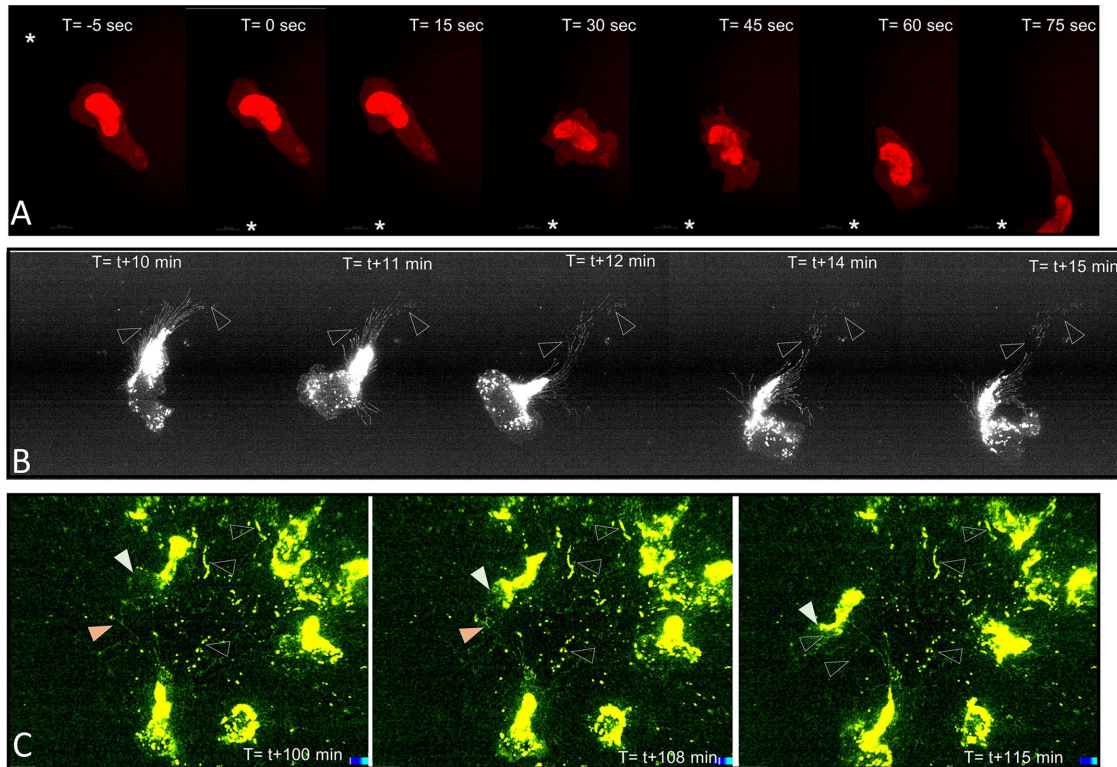


**FIGURE 2:** Experimental support of modeling parameters. (A) Reorientation of migrating differentiated HL-60 cells in response to repositioning of an fMLP-containing micropipette. The cells express mCherry-tagged 5-lipoxygenase, a key LTB<sub>4</sub> synthesizing enzyme, which was used to mark the nucleus. White asterisks mark the position of the micropipette. Also see Supplemental Movie S1. (B) Release of exosomes from migrating cells. Time lapse iSIM super resolution microscopy of differentiated HL-60 cells expressing the exosomal marker CD63 tagged with GFP. Deposition of CD63 positive exosome trails is marked by arrows. Also see Supplemental Movie S2. At the time of addition of fMLP,  $T = 0$ . (C) CD63-GFP expressing cells migrating 2 h post initiation of migration showing CD63 positive vesicular trails. White closed arrow shows position of a migrating cell with respect to exosome trail showed by orange closed arrow. Open arrows show positions of clusters of exosomes over the course of the movie. Also see Supplemental Movie S3.

neutrophil samples the fMLP and LTB<sub>4</sub> concentrations at a given position in the gradient. After sampling, the neutrophil is oriented with the gradient based on the differential receptor occupancy (DFRO), which is the difference in the fraction of ligand-bound receptors across the length of the moving cell. The probability that a cell is oriented toward or away from the gradient is a function of DFRO; the higher the DFRO, the more likely the cell is to be oriented with the gradient. It is assumed that, over the course of the time step, neutrophils move at a constant speed in new directions. The fMLP concentration also controls the rate at which each neutrophil secretes LTB<sub>4</sub>- and LTB<sub>4</sub>-containing exosomes (Figure 1). LTB<sub>4</sub> secretion (directly and through exosomes) causes LTB<sub>4</sub> levels to increase, offset by diffusion and dissipation. This cycle repeats, with neutrophils responding to the fMLP and LTB<sub>4</sub> gradients they experience at their new positions.

### Parameters

The baseline parameters we used are shown in Table 1. Many of these values are well known, namely the length, migration speed, and persistence time of neutrophils. Rather than directly specifying values for the LTB<sub>4</sub> secretion rates ( $\sigma_{CLD}$ ,  $\sigma_{CEO}$ , and  $\sigma_{ELO}$ ) or the cross-sectional area of the simulation domain,  $A$ , we set these values in terms of an overall secretion rate,  $r_L$ , and the fraction of LTB<sub>4</sub> that is secreted via exosomes,  $\phi_E$ . We report results for  $r_L$  varying over

several orders of magnitude and  $\phi_E$  having values between 0 and 1. Concentrations of fMLP and LTB<sub>4</sub> are normalized by their respective values of  $K_d$ .

### Distribution of fMLP

Unless otherwise mentioned, we consider the distributions of fMLP to be exponential,

$$F = \exp\left(-\frac{x-x_0}{\ell_F}\right) \quad (1)$$

where  $F$  is the concentration of fMLP and  $x_0$  is the position in the simulation domain at which the fMLP concentration is 1 (in units of  $K_d$ ). We focus on exponential distributions because, compared with linear gradients, not only are they more representative of gradients that are likely to form in vivo (Oates *et al.*, 2009; Wartlick *et al.*, 2009) but also, as will be discussed later, they are necessary for signal relay to be observed (also see Figure 3). The characteristic length,  $\ell_F$ , represents how shallow or steep an exponential curve is; specifically, it is the distance over which the concentration decreases by a factor of  $1/e$ . The characteristic length of gradients formed by formyl peptides in vivo has not been measured; the value we use corresponds to the length scale of gradients that form in the under-agarose assay (Lauffenburger and Zigmond, 1981; Uden *et al.*, 1986).

Symbol	Parameter	Value
$N$	Number of cells	500
$\sigma_{CL0}$	Maximum LTB <sub>4</sub> secretion rate per cell	Varies
$\sigma_{CE0}$	Maximum exosome secretion rate per cell	Varies
$\sigma_{ELO}$	Maximum LTB <sub>4</sub> secretion rate per exosome	1 K <sub>d</sub> /min per exosome
$F_L$	fMLP concentration leading to half-maximal LTB <sub>4</sub> secretion rate	10 K <sub>d</sub>
$F_E$	fMLP concentration leading to half-maximal exosome secretion rate	10 K <sub>d</sub>
$\ell_F$	Characteristic length of fMLP gradient	400 μm
$\gamma_E$	Exosome activity decay rate	0.01/min
$D_L$	LTB <sub>4</sub> diffusion coefficient	$2.4 \times 10^4$ μm <sup>2</sup> /min
$\gamma_L$	LTB <sub>4</sub> dissipation rate	0.27/min
$A$	Cross-sectional area for diffusion	
$\ell_V$	Length of volume in which cells migrate	10 mm
$\ell_C$	Neutrophil length	10 μm
$v$	Neutrophil speed	10 μm/min
$\Delta t$	Neutrophil persistence time	1 min
$S_F$	Sensitivity of neutrophils to fMLP	200
$S_L$	Sensitivity of neutrophils to LTB <sub>4</sub>	200
$F_{xt}$	fMLP-induced desensitization to LTB <sub>4</sub>	1 K <sub>d</sub>

**TABLE 1:** Model parameters.

### fMLP-induced LTB<sub>4</sub> and exosome secretion rates

A neutrophil secretes LTB<sub>4</sub> (directly) and exosomes (that contain LTB<sub>4</sub>) at rates  $\sigma_{CL}$  and  $\sigma_{CE}$ , respectively. These rates are assumed to vary with  $F$  as

$$\sigma_{CL} = \sigma_{CL0} \frac{F}{F + F_L} \quad (2)$$

and

$$\sigma_{CE} = \sigma_{CE0} \frac{F}{F + F_E} \quad (3)$$

Here  $\sigma_{CL0}$  is the maximum LTB<sub>4</sub> secretion rate and  $\sigma_{CE0}$  is the maximum rate of secretion of exosomes by a neutrophil. We treat these secretion rates as functions only of the fMLP concentration (per Eq. 1) and not otherwise varying in time. Although neutrophils secrete exosomes and LTB<sub>4</sub> at time-varying rates even at fixed fMLP concentrations, we neglect this for the sake of simplicity.

### Exosome activity distribution

In the following section, we provide an equation for the rate of change of local LTB<sub>4</sub> concentration, in which exosome distribution is represented as a function of position and time. Two considerations have been taken into account in modeling exosome distribution and activity. First, a large number of exosomes would be secreted by a population of neutrophils over the simulation period, so it is not feasible to represent each exosome individually. Second, given that exosomes can only release a finite amount of LTB<sub>4</sub>, the model should account for the fact that exosomal secretion of LTB<sub>4</sub> occurs at a time-decaying rate.

We assume that the secretion of LTB<sub>4</sub> by an exosome follows exponential decay; that is, the secretion rate of a single exosome is

$$\sigma_{EL} = \sigma_{ELO} \exp(-\gamma_E(t - \tau)), \quad (4)$$

where  $\sigma_{ELO}$  is the initial rate at which the exosome secretes LTB<sub>4</sub> and  $\tau$  is the time at which the exosome is expelled from a cell. Therefore, rather than tracking each exosome, we track the distribution of

“exosome activity,”  $E(x)$ , which is the concentration of exosomes adjusted for decaying LTB<sub>4</sub> content. The exosome activity distribution varies according to

$$\frac{dE}{dt} = -\gamma_E E + \frac{1}{A} \sum_{k=1}^N \delta_h(x - X_k) \sigma_{CE,k} \quad (5)$$

where  $\gamma_E$  is the rate at which LTB<sub>4</sub> secretion by exosomes decreases. Note that we consider LTB<sub>4</sub> diffusion to occur in one dimension in a volume of length  $\ell_V$  and cross-sectional area  $A$ . The number of cells in that volume is  $N$ . The  $k$ th neutrophil has an fMLP-dependent exosome secretion rate of  $\sigma_{CE,k}$  and is at position  $X_k$ . We track exosome activity levels in finite bins of width  $h = 10$  μm, which is close to the size of a typical neutrophil. Based on experimental data, we assume that exosomes remain where they are secreted (for times comparable to  $1/\gamma_E$  and other relevant kinetic parameters). In Supplemental Movie S2 and Figure 2B, migrating HL-60 cells (expressing a GFP tagged exosomal marker CD63) release vesicles that do not appear to diffuse after their release. Furthermore, the deposition of vesicles seems to be a stable event as trails of CD6-positive vesicles are still visible 2 h after the initiation of migration (Figure 2C and Supplemental Movie S3).

The discrete Dirac delta,  $\delta_h$ , which represents how the exosomes secreted by a neutrophil add to the activity in the bin that the neutrophil currently occupies, is approximated as

$$\delta_h(r) = \begin{cases} 1/h, & |r| \leq h \\ 0, & \text{otherwise} \end{cases} \quad (6)$$

### Modeling rate variation of LTB<sub>4</sub> from cells and exosomes

The local rate of change of LTB<sub>4</sub> concentration is given by a reaction-diffusion equation,

$$\frac{dL}{dt} = D_L \frac{d^2L}{dx^2} - \gamma_L L + \sigma_{ELO} E + \frac{1}{A} \sum_{k=1}^N \delta_h(x - X_k) \sigma_{CL,k} \quad (7)$$

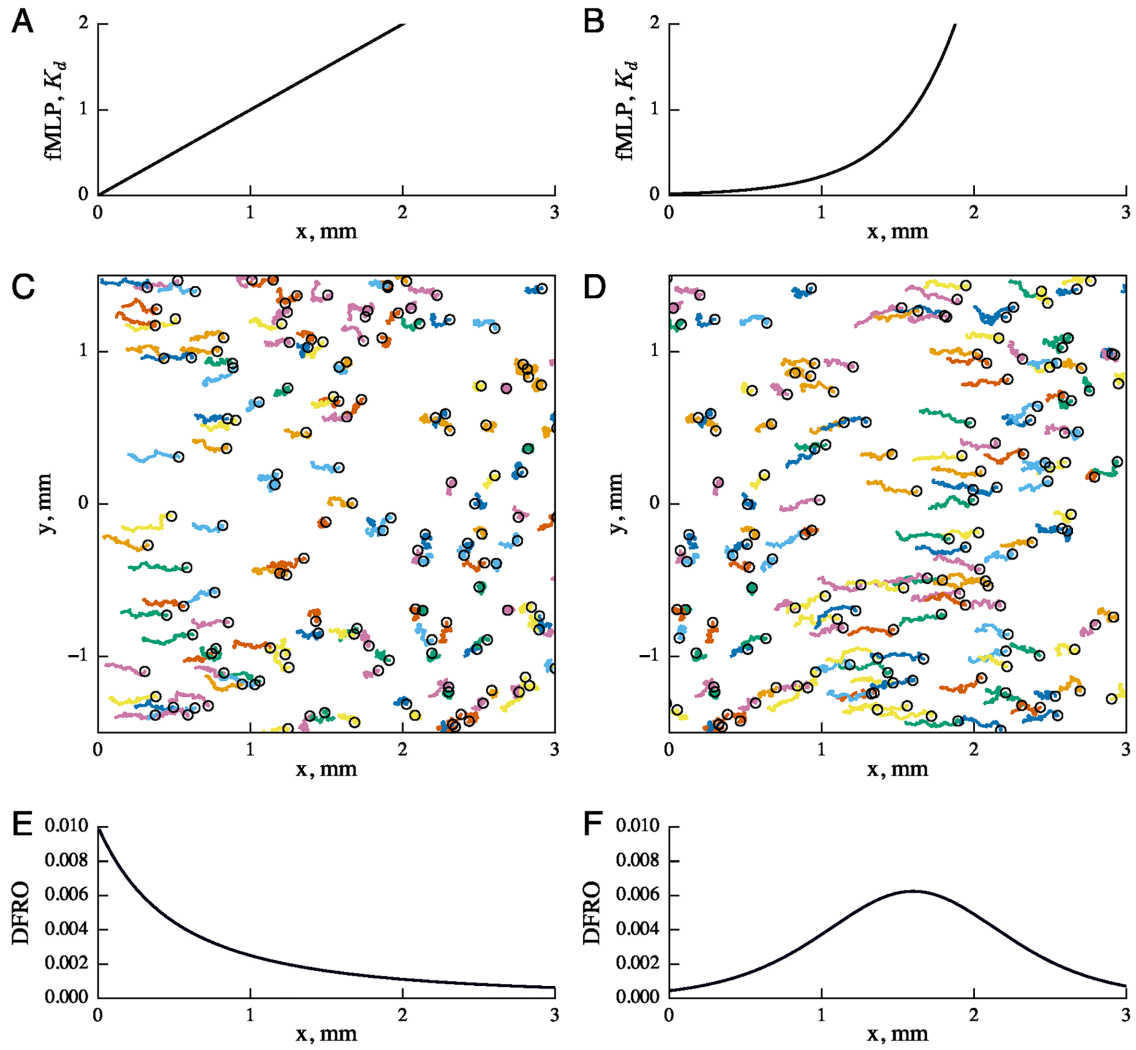


**FIGURE 3:** Cell motility in linear or exponential gradients governed by differential receptor occupancy. Cells were subjected to linear (A) or exponential (B) gradients of fMLP. For exponential gradients, the concentration of fMLP increased by a factor of  $e$  every 400  $\mu\text{m}$  (see Eq. 1). Colored tracks show motion of individual neutrophils, simulated for 1 h in a linear gradient (C) and in an exponential gradient (D); final positions are shown as circles. Results are shown for a 3-mm segment in the middle of a 10-mm simulation domain. (E, F) DFRO (see Eq. 11). A cell would have a higher DFRO where the gradient is steep but the concentration is not saturating. Higher DFRO causes the orientation distribution of cells to be biased in the direction of increasing chemoattractant concentration.

where  $L$  is the concentration of  $\text{LTB}_4$  at point  $x$  and  $D_L$  is the diffusion coefficient for  $\text{LTB}_4$ . Similarly to Eq. 5, the  $k$ th neutrophil has an fMLP-dependent free  $\text{LTB}_4$  secretion rate of  $\sigma_{CE,k}$ . Exosomes secrete  $\text{LTB}_4$  at a rate of  $\sigma_{CE0}$ , and the  $\text{LTB}_4$  concentration in the medium is assumed to decrease intrinsically (other than by diffusion) at a rate of  $\gamma_L$  due to various mechanisms, including perhaps aggregation or adsorption to the extracellular matrix. Under *Materials and Methods*, we describe how we solve Eqs. 5 and 7, linking results to secretion rates in terms of an overall  $\text{LTB}_4$  secretion rate,  $r_L$ , and the fraction of  $\text{LTB}_4$  that is secreted via exosomes,  $\phi_E$ ; these were the two main parameters that we varied directly. The concentrations of  $\text{LTB}_4$  that cells sense are determined by the total rate at which cells secrete  $\text{LTB}_4$  (directly and via exosomes) and by how much space  $\text{LTB}_4$  can be diluted into. If each cell were secreting at the maximum rate possible, and the loss of  $\text{LTB}_4$  were negligible ( $\gamma_L = 0$ ), then the  $\text{LTB}_4$  concentration would tend to increase at the rate

$$r_L = \frac{(\sigma_{CLO} + \sigma_{CE0}\sigma_{ELO} / \gamma_E)N}{A\ell_V} \quad (8)$$

In this expression, the contribution from exosomes,  $\sigma_{CE0}\sigma_{ELO} / \gamma_E$ , implicitly assumes that each exosome secretes a finite amount of  $\text{LTB}_4$ , at a rate that decays over time. The fraction of  $\text{LTB}_4$  secreted via exosomes is given by

$$\phi_E = \frac{\sigma_{CE0}\sigma_{ELO} / \gamma_E}{\sigma_{CLO} + \sigma_{CE0}\sigma_{ELO} / \gamma_E} \quad (9)$$

and can vary from 0 (all  $\text{LTB}_4$  is secreted directly) to 1 (all  $\text{LTB}_4$  is secreted via exosomes).

$\text{LTB}_4$  gradients have not been measured directly but arachidonic acid (AA), the precursor to  $\text{LTB}_4$ , was observed to move a shorter distance than fMLP (Uden *et al.*, 1986). However, if  $\text{LTB}_4$  moved as a freely diffusing monomer, it should diffuse farther than fMLP, due to its lower molecular weight. Observed AA distributions

(Uden *et al.*, 1986) resemble predictions for hindered gradients—gradients that evolve by diffusion but with molecules adsorbed onto surfaces (Dahlgren *et al.*, 1984). Because LTB<sub>4</sub> is a lipid-derived hydrophobic molecule, it could bind to surfaces or form micelles or aggregates; it could also bind to diffusible carrier proteins. For the sake of simplicity, we account for these effects by treating LTB<sub>4</sub> concentration as decreasing with first-order kinetics at a rate  $\gamma_L$ . Based on its molecular weight, we assume that LTB<sub>4</sub> has a diffusion coefficient  $D_L = 2.4 \times 10^4 \mu\text{m}^2/\text{min}$ . This yields a characteristic length for LTB<sub>4</sub> gradients of  $\ell_L = \sqrt{D_L / \gamma_L}$ : in a simple exponential gradient generated by a single source secreting LTB<sub>4</sub>,  $\ell_L$  is the distance over which the LTB<sub>4</sub> concentration increases by a factor of e. To approximately match LTB<sub>4</sub> distributions measured previously (Uden *et al.*, 1986; Foxman *et al.*, 1997), we set  $\gamma_L = 0.27/\text{min}$  so  $\ell_L = 300 \mu\text{m}$ .

### Modeling directed cell motion guided by evolving chemoattractant gradients

Directional sensing biases the movement of neutrophils toward the direction of increasing chemoattractant concentration. Based on current evidence, the change in receptor occupancy across the length of the cell is the best predictor of cell bias. The fractional receptor occupancy (FRO) at a point on the cell surface is

$$\text{FRO} = \frac{c}{c + K_d} \quad (10)$$

where  $c$  is the chemoattractant concentration at the surface and  $K_d$  is the dissociation coefficient for the chemoattractant-receptor interaction. The DFRO across the length of the cell is obtained by taking the derivative of FRO with respect to  $x$  (the direction in which concentration varies), and scaling by the length,  $\ell_C$ , of the cell,

$$\text{DFRO} = \frac{\ell_C}{K_d} \frac{dc}{dx} \frac{1}{(c/K_d + 1)^2} \quad (11)$$

This is approximately equal to the difference in fractional receptor occupancy between the points on the cell located farthest up and farthest down the gradient. DFRO has been shown to be roughly proportional to the chemotactic index or mean cell velocity for a variety of cell types, including neutrophils (Tranquillo *et al.*, 1988; Herzmark *et al.*, 2007), dendritic cells (Haessler *et al.*, 2011; Wang and Irvine, 2013), T-cells (Wang and Irvine, 2013), and breast cancer cells (Kim *et al.*, 2013). There are a variety of sources of noise that interfere with chemotaxis, including stochastic binding of chemoattractants to the receptors (Berg and Purcell, 1977) amplification of gradient signals and conversion of those signals into cell motion. Rather than accounting for each of these complex processes separately, we use DFRO to determine a realistic overall level of noise.

In our model, both fMLP and LTB<sub>4</sub> can direct neutrophils, but when a cell senses fMLP its sensitivity to LTB<sub>4</sub> decreases. We represent the combined gradient signal,  $\kappa$ , as a weighted sum of the DFRO for each gradient,

$$\kappa = S_F \text{DFRO}_F + S_L \exp(-F/F_{xt}) \text{DFRO}_L \quad (12)$$

where  $S_F$  and  $S_L$  are the sensitivities of neutrophils to gradients of fMLP and LTB<sub>4</sub>, respectively. The exponential term in this expression accounts for neutrophils being less sensitive to LTB<sub>4</sub> when they can sense fMLP (Heit *et al.*, 2002), with  $F_{xt}$  being the fMLP concentration leading to an e-fold decrease in LTB<sub>4</sub> sensitivity.

Under *Materials and Methods*, we describe how we estimated the sensitivities  $S_F$  and  $S_L$ . Neutrophils favor formyl peptides over

intermediate chemoattractants such as LTB<sub>4</sub> (Heit *et al.*, 2002); therefore, we adjusted  $F_{xt}$  to be just low enough that we did not observe cells migrating up an LTB<sub>4</sub> gradient when opposed by an fMLP gradient under normal conditions. At each time step, the direction of neutrophil locomotion was determined by a biased random process, such that higher  $\kappa$  values make it more likely that the neutrophil is aligned with the gradient. The neutrophil then moves in this direction at a speed  $v$  for a period  $\Delta t$ . After that point, the steps shown in Figure 1 repeat.

## RESULTS

### Exponential chemoattractant gradients direct cell migration better than linear gradients

We first investigated cell response to two fMLP gradient shapes: a linear gradient (Figure 3A) and an exponential gradient (Figure 3B) with a characteristic length  $\ell_F = 400 \mu\text{m}$  (see Eq. 1). As seen in Figure 3C, in a linear gradient the cells were most strongly directed in areas with low concentrations ( $<1 \text{ mm}$ ). In contrast, for exponential gradients, the cells were most directed in areas where the concentration was near the  $K_d$  (in Figure 3D, roughly 1–2 mm, with concentration ranging from 0.3 to 3.5  $K_d$ ). This difference in directed cell motion is due to differences in where cells have high DFRO (Figure 3, E and F). In a linear gradient, DFRO is highest where the concentration is lowest (Figure 3E). In contrast, DFRO is highest in an exponential gradient where the concentration is approximately the  $K_d$  (Figure 3F). These findings agree with the observations by Herzmark *et al.* (2007) showing that chemotactic index is highest at the low concentration end of a linear gradient or in the part of an exponential gradient where the concentration is close to  $K_d$ . We find that, although the maximum DFRO is higher in the linear gradient, an effective DFRO ( $>0.005$ ) is sustained over a greater spatial range in the exponential gradient. As signal relay extends the spatial range over which cells can be directed, it is necessary that we model neutrophils in conditions where the gradient signal is weak far from a chemoattractant source. We focus on neutrophil response to exponential gradients because, in exponential gradients, signal relay could potentially attract cells in areas where the slope of the gradient is shallow. In linear gradients, the slope is uniform; variation in directionality arises from high concentrations leading to saturation of chemoattractant receptors. Therefore, as stated under *Model*, we used an exponentially decaying gradient of fMLP for all other simulations.

### LTB<sub>4</sub> mediates signal relay in chemotactic neutrophils

We previously established a role for LTB<sub>4</sub> signal relay during neutrophil chemotaxis by mixing wild-type (WT) neutrophils with neutrophils that cannot sense fMLP (Afonso *et al.*, 2012; Majumdar *et al.*, 2016). We showed that the migration defects of neutrophils that do not have functional formyl peptide receptors (FPR) can be rescued by mixing them with WT neutrophils that are capable of producing LTB<sub>4</sub>. This fundamental behavior, central to the concept of signal relay, is recapitulated by our model in Figure 4. We show that WT neutrophils migrating in an fMLP gradient (Figure 4A) exhibit robust chemotaxis (Figure 4D) and secrete LTB<sub>4</sub> (Figure 4G), while cells lacking FPR show neither chemotaxis (Figure 4E) nor LTB<sub>4</sub> production under similar conditions (Figure 4H). When combined with WT neutrophils, neutrophils lacking FPR regain the ability to chemotax (Figure 4F) by detecting the LTB<sub>4</sub> gradient created by the WT neutrophils (Figure 4I). The shape of the resultant LTB<sub>4</sub> gradient remains similar to that of the original gradient (Figure 4, A and G).

We studied the effect of signal relay on populations of cells migrating in response to fMLP by comparing the migration of cells

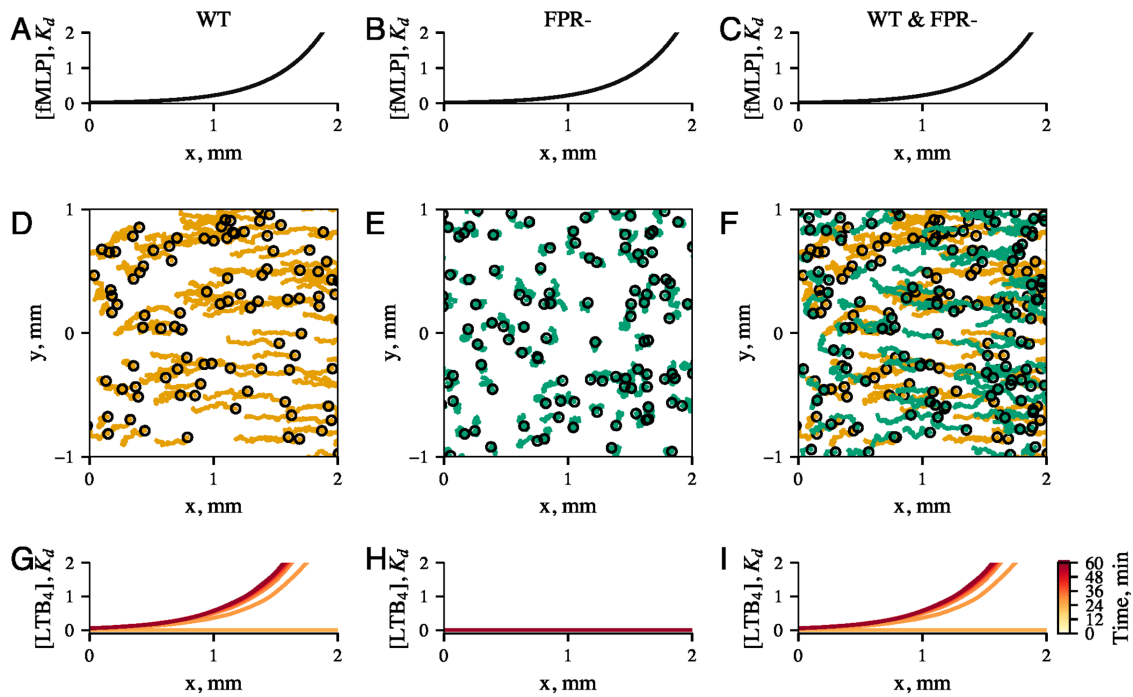


**FIGURE 4:** Migrating neutrophils generate an  $LTB_4$  gradient that recruits other neutrophils. Cell migration and secreted  $LTB_4$  profile of (A) WT neutrophils that can sense fMLP, (B) FPR neutrophils that cannot, and (C) FPR neutrophils combined with WT cells. (A–C) Concentration profiles of fMLP. (D–F) Tracks showing motion of simulated neutrophils that can sense fMLP (WT, orange) and neutrophils that cannot (FPR, green); final positions are shown as circles. The cells that sense fMLP generate a gradient of  $LTB_4$  which directs the cells that cannot sense fMLP. (G–I) Concentration profiles of secreted  $LTB_4$ ; darker curves indicate concentrations at later times. The overall concentration of  $LTB_4$  increases over time. This data show 1 h of simulated time, with  $r_L = 4 K_d/\text{min}$ .

incapable of detecting  $LTB_4$ , and hence defective in signal relay (BLT-, Figure 5, left), with the migration of  $LTB_4$ -sensitive cells capable of signal relay (BLT+, Figure 5, right). As shown in Figure 5, C and D, while both BLT- and BLT+ cells responded in the steep parts of gradients, only the BLT+ cells were capable of directed cell migration in regions where the primary fMLP gradient is too shallow for effective chemotaxis ( $<0.002 K_d/\mu\text{m}$ ), shown here as a shaded region. This indicates that signal relay increases the spatial range over which cells can be recruited. Together, these findings show that our model faithfully recapitulates the biological process of  $LTB_4$  signal relay during neutrophil chemotaxis.

### Exosomes regulate the evolution of $LTB_4$ gradients and control the time required to reach equilibrium concentrations

We next sought to explain how packaging of  $LTB_4$  in exosomes and its subsequent release affects the evolution of  $LTB_4$  gradients and how, in turn, this affects directed cell motion. For purposes of comparison, we set  $LTB_4$  secretion rates such that, on fMLP stimulation, cells secrete  $LTB_4$  at the same rate regardless of whether the  $LTB_4$  is secreted directly or is packaged in exosomes. Figure 6 shows how cell response differs if  $LTB_4$  is secreted via exosomes (right panel) rather than directly (left panel). When  $LTB_4$  is gradually released from exosomes, the time taken for the  $LTB_4$  profile to reach steady state is subject to the decay rate of the exosomal  $LTB_4$  (Figure 6E), and high  $LTB_4$  secretion rates are not reached until 1 h into the simulations (Figure 6G). In contrast, an equilibrium profile is reached within 6 min if  $LTB_4$  is secreted directly (Figure 6F). We assume that when cells directly secrete  $LTB_4$ , it is immediately available to affect cell motion, whereas when cells secrete  $LTB_4$ -containing exosomes, the exo-

somes then gradually secrete the  $LTB_4$ . To characterize the effect of the profiles on the behavior of the cells, we calculated the directionality of the cells. We define “directionality” as the mean of the cosine of the orientation angles that cells would have at a given time and position, as determined by the biased distribution of cell orientations in response to the chemoattractant gradient (given by Eq. 12). This is comparable to the chemotactic index, but, while the chemotactic index is used to measure the directed motion of cells over time, we use directionality to capture the average motion of cells at a particular time and position. As shown in Figure 6, H and I, directionality reaches its maximum value more rapidly for direct rather than exosomal secretion. Therefore, secretion of  $LTB_4$  via exosomes can mediate signal relay similarly to direct secretion of  $LTB_4$ , but relay begins more gradually. Thus, exosomes may play a critical role in pathological conditions such as sepsis, where large quantities of  $LTB_4$  are expected to be released into tissues and saturate cell surface receptors. By gradually releasing  $LTB_4$ , exosomes may prevent  $LTB_4$  profiles from rapidly reaching such saturating concentrations.

### Maximum range of cell recruitment occurs at intermediate $LTB_4$ secretion rates and is dependent on exosomal secretion

We next quantified the effect of signal relay on the distance over which cells can be recruited. For this purpose, we define the recruitment range as the length of the zone over which directionality is at least 0.5. Data were obtained from simulations conducted with a wide range of  $LTB_4$  secretion rates,  $r_L$  (see Eq. 8). We also varied the fraction of  $LTB_4$  that is secreted by being packaged into exosomes,  $\phi_E$ : on secretion, the exosomes gradually release  $LTB_4$  (per Eq. 4). As seen in Figure 7A, the recruitment range was calculated to be

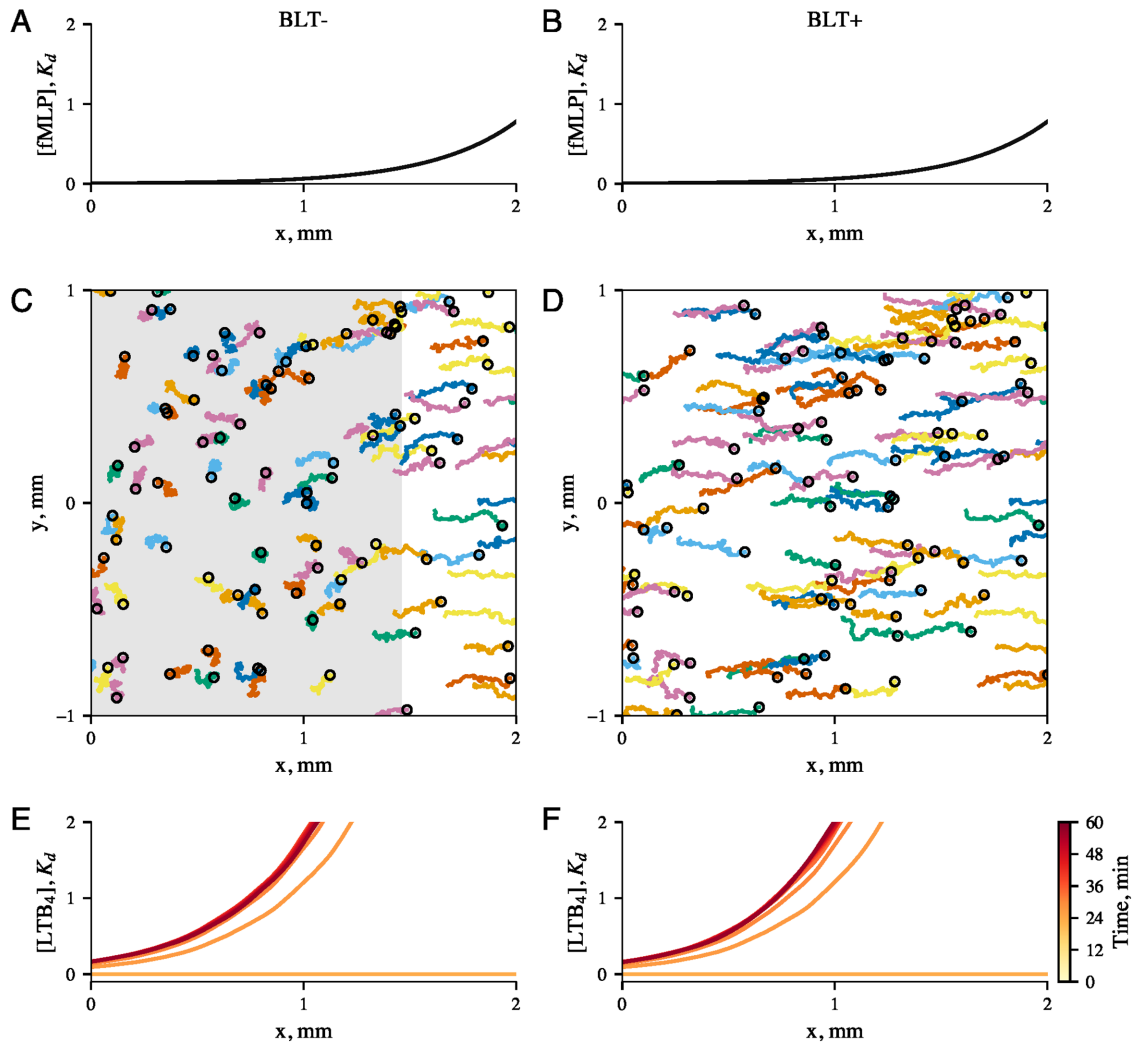


**FIGURE 5:** Signal relay enhances group migration of neutrophils. Neutrophil migration is shown for cells without (left) and with (right) BLT, a receptor for LTB<sub>4</sub>. (A, B) Concentration of fMLP, the primary chemoattractant as a function of position. (C, D) Tracks showing motion of neutrophils over 1 h; final positions are shown as circles. When relay is disabled (left), cells in the shaded region cannot sense the fMLP gradient as it is too shallow at that position. However, in the case when cells relay signals (right), cells in the shallow part of the fMLP gradient can undergo directed motion. (E, F) Concentration of LTB<sub>4</sub>, the secondary chemoattractant; darker colors indicate later time points; profiles are shown for time points at 6-min intervals, over a period of 1 h, with  $r_L = 4 K_d/\text{min}$ .

0.43 mm for no, or extremely low, LTB<sub>4</sub> secretion ( $r_L < 10^{-2} K_d/\text{min}$ ). We calculated the recruitment range at 1 h after the start of the simulation, which is enough time for gradients to form but still brief enough to be physiologically relevant.

The model predicts that LTB<sub>4</sub>-mediated relay increases the range up to threefold, which agrees qualitatively with experimental results (Lämmermann *et al.*, 2013). For signal relay to increase the recruitment range, LTB<sub>4</sub> must be secreted at an intermediate rate ( $r_L \approx 10\text{--}100 K_d/\text{min}$ ). At moderate rates (Figure 7B, middle panel) the recruitment range is extended by a strong LTB<sub>4</sub> signal generated where the fMLP gradient is too shallow to sense (Figure 7B, v). The recruitment range strongly depends on  $r_L$  and is shorter at low or high secretion rates. For low secretion rates (Figure 7B, left panel), LTB<sub>4</sub> does not appreciably increase the recruitment range (Figure 7B vii) because in regions where the fMLP gradient is too shallow for cells to sense, the LTB<sub>4</sub> gradient is even shallower, yet, in the steeper part of the fMLP gradient, the high concentration of fMLP diminishes the sensitivity of the cell to the LTB<sub>4</sub>. For very high LTB<sub>4</sub> secre-

tion rates, the directionality is high in two different regions (Figure 7B, ix), one dominated by the LTB<sub>4</sub> gradient and another due to the fMLP; signal relay would not be useful under these circumstances.

To understand how the secretion of LTB<sub>4</sub> by exosomes affects recruitment range, we varied  $\phi_E$ , the fraction of LTB<sub>4</sub> secreted from exosomes (Eq. 9). LTB<sub>4</sub> can be secreted directly ( $\phi_E = 0$ ), entirely via exosomes ( $\phi_E = 1$ ), or by a combination of the two modes of secretion ( $0 < \phi_E < 1$ ). The maximum recruitment range is not very different when LTB<sub>4</sub> is either released directly ( $\phi_E = 0$ ), or released exclusively from exosomes ( $\phi_E = 1$ ) and remains around 1.5–1.7 mm (Figure 7A). The main overall difference in recruitment range due to direct or exosomal secretion of LTB<sub>4</sub> is that for a higher release rate ( $r_L$ ), an optimal recruitment range is obtained if a greater fraction of LTB<sub>4</sub> is released via exosomes (higher  $\phi_E$ ). This effect is due to the time delay involved in exosomal secretion, as mentioned in the previous section. For a given  $r_L$ , the amount of LTB<sub>4</sub> in solution at 1 h is higher for direct secretion. At that point, with exosome-mediated LTB<sub>4</sub> secretion, much of the LTB<sub>4</sub> is still contained in exosomes and

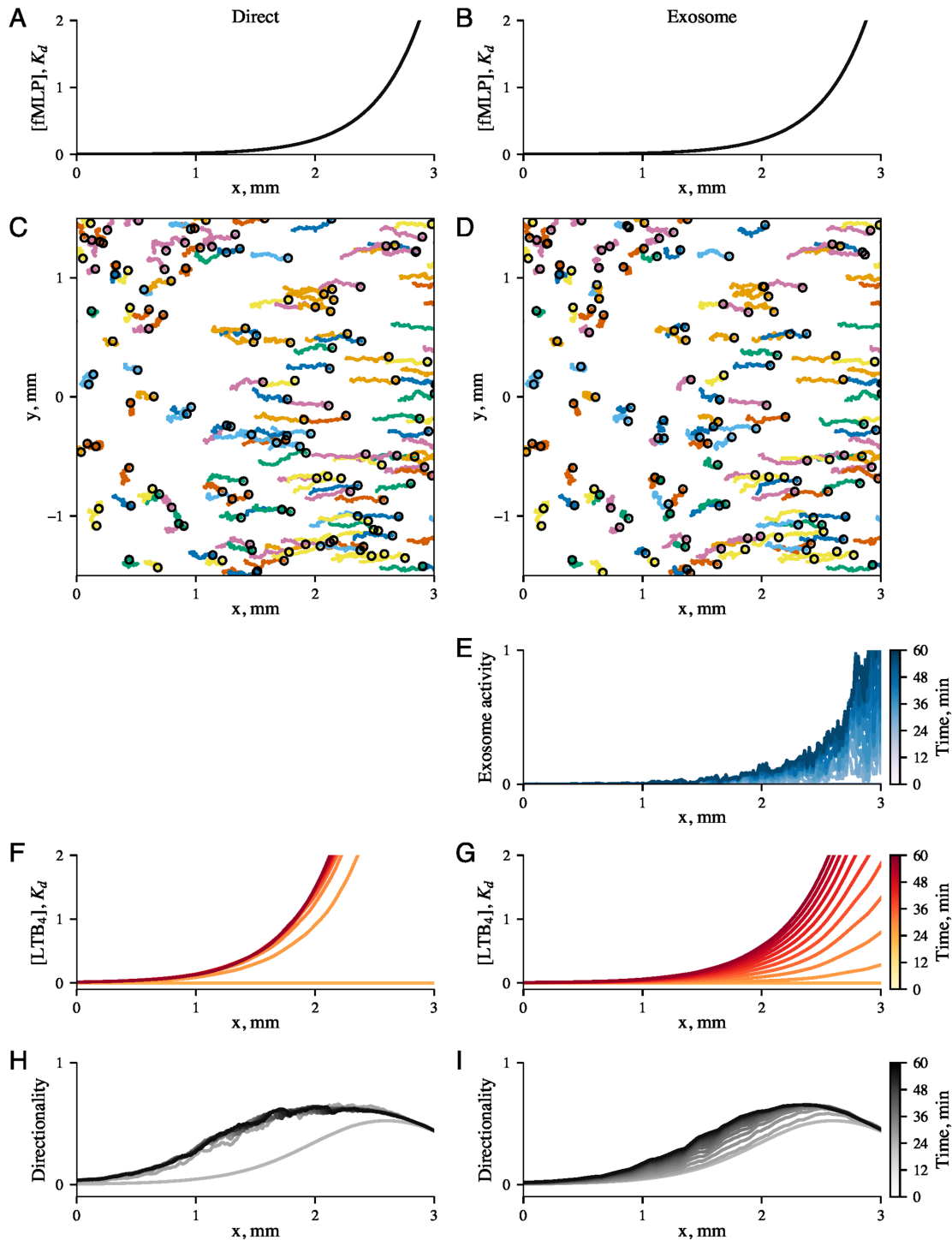


**FIGURE 6:** Under steady-state fMLP conditions, LTB<sub>4</sub> gradients require more time to develop when released through exosomes, as compared with direct secretion from cells. Collective response of neutrophils signaling by secreting LTB<sub>4</sub> directly (left panel) or via exosomes (right panel). (A, B) Concentration of the primary chemoattractant, fMLP, as a function of position. (C, D) Tracks showing motion of neutrophils; final positions are shown as circles. (E) Exosome activity, that is, the rate of LTB<sub>4</sub> secretion via exosomes. (There is no exosome activity in the case shown in the left column.) (F, G) Concentration profile of released LTB<sub>4</sub>. (H, I) Directionality of migrating cells. Curves displayed in E–I show levels at 6-min increments over a total simulation time of 1 h. The value  $r_L = 4 K_d/\text{min}$  was used. Darker colors indicate later time points.

cannot be sensed by cells. Therefore, exosome-mediated secretion keeps LTB<sub>4</sub> concentrations from rising too high in response to primary chemoattractants during the initiation of an inflammatory phase.

### Exosomes stabilize LTB<sub>4</sub> gradients under conditions of time-decaying primary chemoattractant gradients

For rapid inflammatory pathophysiological conditions, such as injury, ischemia, or during the early onset of infection, the concentration

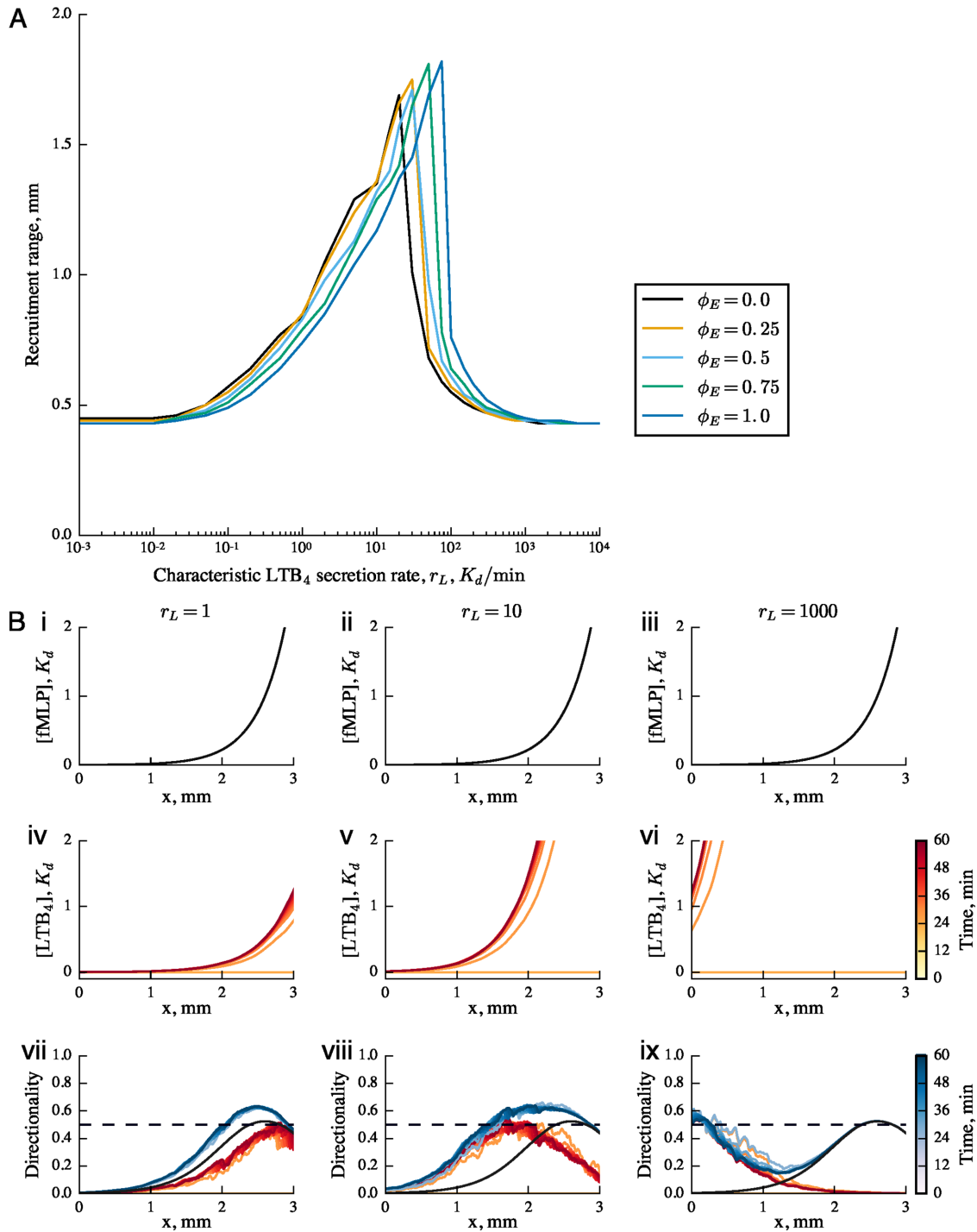


**FIGURE 7:** Signal relay via LTB<sub>4</sub> increases the recruitment range, the distance over which cells can be oriented by a gradient. (A) Recruitment ranges are shown for times 1 h after the start of the simulations. Recruitment range is plotted as a function of the normalized LTB<sub>4</sub> secretion rate,  $r_L$ , for several values of the fraction of LTB<sub>4</sub> that is secreted via exosomes,  $\phi_E$ . When  $\phi_E = 1$ , LTB<sub>4</sub> is secreted entirely via exosomes, while if  $\phi_E = 0$ , LTB<sub>4</sub> is secreted directly by the cells. (B) Moderate LTB<sub>4</sub> secretion rates are necessary for the recruitment range to be increased. Concentrations of fMLP (i–iii) and LTB<sub>4</sub> (iv–vi), as well as directionality (vii–ix), are shown for secretion rates ( $r_L$ ) of 1 (i, ix, vii), 10 (ii, v, viii), and 1000  $K_d/\text{min}$  (iii, vi, ix). The plots of directionality show total directionality (blue), as well as the directionality that would result if cells were to perceive only fMLP (black) or LTB<sub>4</sub> (red). Curves displayed show levels at 6-min increments over a total simulation time of 1 h; darker colors indicate later time points.

of primary chemoattractants, such as formylated peptides belonging to damage-associated molecular patterns (DAMPs), is expected to rise rapidly in the tissue followed by gradual decay in concentration (Land, 2015). We modeled this by subjecting neutrophils to an

fMLP gradient for 1 h and then causing the fMLP concentration to decay exponentially at a rate of 0.2/min. Figure 8, C and D, shows results as a function of time for the first 1 h after the fMLP gradient begins to decay. When LTB<sub>4</sub> is secreted directly, the LTB<sub>4</sub> profile

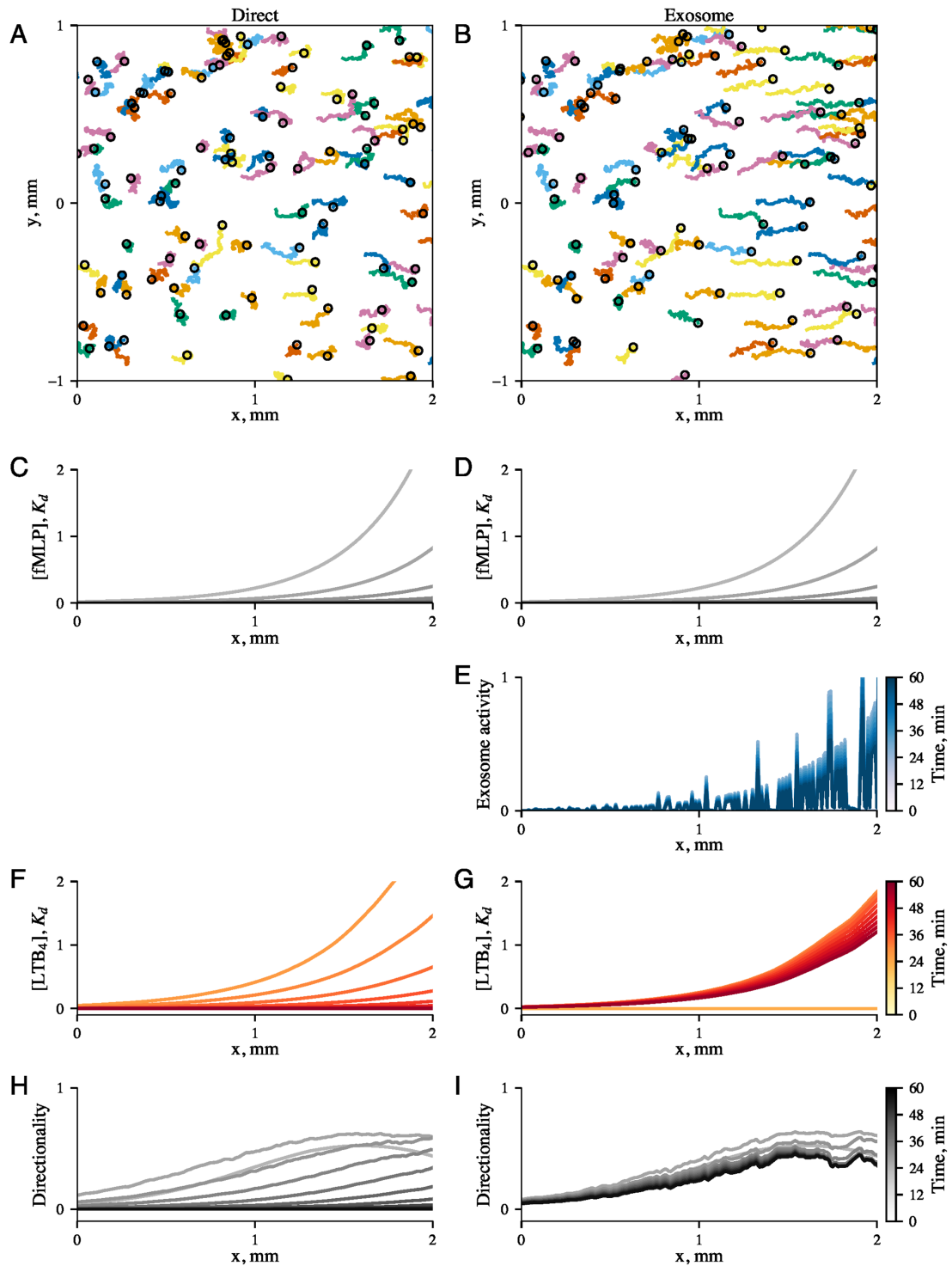


**FIGURE 8:** Exosomes prolong directionality of cell migration in decaying fMLP gradient. Results shown for neutrophils secreting  $LTB_4$  directly (left panel) or via exosomes (right panel). (A, B) Tracks showing motion of neutrophils; final positions are shown as circles. (C, D) Concentration of the primary chemoattractant, fMLP; concentration decreases exponentially at a rate of  $0.2 \text{ min}^{-1}$ . Curves from later time points are shown in progressively darker shades. (E) Exosome activity, that is, the rate of  $LTB_4$  secretion via exosomes. (There is no exosome activity in the case shown in the left column.) (F, G) Concentration of  $LTB_4$ . (H, I) Directionality of migrating cells. Curves displayed in C–I show levels at 6 min increments over a total simulation time of 1 h. A value of  $r_L = 4 \text{ K}_d/\text{min}$  was used. Darker colors indicate later time points.

mimics the time-varying fMLP profile (Figure 8F), which falls rapidly, causing a decrease in directionality and recruitment of other neutrophils (Figure 8H). In contrast, when  $LTB_4$  is secreted via exosomes, directed migration is maintained. This is because the early fMLP

profile causes exosomes to be predominantly secreted in areas with high fMLP concentration (Figure 8E). As the fMLP concentrations fall, the rate at which cells secrete exosomes decreases; even so, in comparison with direct  $LTB_4$  secretion, the rate at which  $LTB_4$  enters

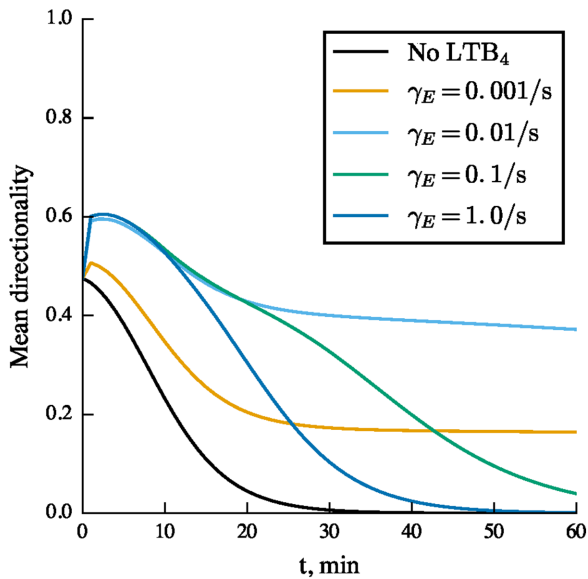


**FIGURE 9:** Directed migration is best preserved if exosomes release  $\text{LTB}_4$  at an intermediate rate. Mean cell directionality in a  $1\text{ mm} \times 1\text{ mm}$  simulation area is shown for cells when the fMLP gradient decays (see Figure 8), as a function of time for various exosomal  $\text{LTB}_4$  activity rates.

solution is more stable. Hence, even after the fMLP concentration falls, the  $\text{LTB}_4$  profile is maintained for at least 1 h (Figure 8G). Consequently, with exosomal  $\text{LTB}_4$  secretion, the directionality of cell migration is maintained even in extremely shallow gradients of fMLP (Figure 8I).

To quantify the stabilization of  $\text{LTB}_4$  gradients via exosomal secretion and its effect on directionality, we repeated these simulations for various values of  $\gamma_E$ , the rate at which exosomal secretion of  $\text{LTB}_4$  decays (Figure 9). Our model predicts that intermediate exosomal  $\text{LTB}_4$  secretion rates are best for sustaining directed migration. At a high rate of  $\text{LTB}_4$  secretion (e.g.,  $1.0/\text{s}$ ) directionality drops in the first 30 min because the exosomes rapidly run out of  $\text{LTB}_4$  and, although low levels of  $\text{LTB}_4$  secretion (e.g.,  $0.001/\text{s}$ ) enable  $\text{LTB}_4$  signaling to occur for a relatively long duration, the signal is weak ( $<0.2$  after 20 min). In contrast, an intermediate rate ( $0.01/\text{s}$ ) maintains directionality above 0.4 for more than 1 h.

## DISCUSSION

In our model, a cell migrates by detecting differences in chemoattractant concentrations, implicitly transducing the differences in receptor occupancy into an intracellular gradient, and, finally, migrating in the direction of more ligand-bound receptors. A similar approach has been used previously to model neutrophil motion, employing a “chemotaxis coefficient” to account for DFRO and receptor down-regulation (Tranquillo et al., 1988). In this study, we used DRFO not only to determine the spatial distribution of directions in which cells move but also to account for response to multiple chemoattractants. In agreement with previous experimental findings, our model shows that migrating neutrophils can generate gradients of  $\text{LTB}_4$  that guide neutrophils that cannot sense fMLP. The model can also replicate the finding that impairing  $\text{LTB}_4$ -mediated signal relay decreases the directed motion of neutrophils toward fMLP. In addition, our model shows that exponential gradients are better at directing cell migration than are linear gradients, and, in accordance with existing literature (Afonso et al., 2012; Lämmermann

et al., 2013; Majumdar et al., 2016), that cells with  $\text{LTB}_4$  receptors are more directed in the shallow parts of fMLP gradients than are cells lacking such receptors. Furthermore, our model predicts that  $\text{LTB}_4$ -mediated signal relay acts by extending the range over which cells can be directed (the recruitment range) by a factor of two to three, again reproducing experimental data (Lämmermann et al., 2013). Results show that the recruitment range is maximized for  $r_L$  in the range of 1–100  $K_d/\text{min}$ , which corresponds to rates that are attainable for neutrophils. Indeed, the  $\text{LTB}_4$  secretion rate per neutrophil is related to the secretion rate  $r_L$  divided by the number of neutrophils per unit volume. Assuming that neutrophils are tightly packed, with one neutrophil per  $10\text{-}\mu\text{m}$  cube, the secretion rate that optimizes signal relay is between  $1 \times 10^{-21}$  and  $1 \times 10^{-19}$  moles of  $\text{LTB}_4/\text{min}/\text{neutrophil}$ . The maximum rate at which neutrophils secrete  $\text{LTB}_4$  has been measured to be in the range of  $3 \times 10^{-20}$  to  $3 \times 10^{-17}$  mol  $\text{LTB}_4/\text{min}$  (Afonso et al., 2012). Therefore, neutrophil  $\text{LTB}_4$  secretion rates are adequate to increase the recruitment range. Concentration levels and gradient slopes are linked not just to the secretion rates of individual neutrophils but also by cell density.

Our model shows that, although releasing  $\text{LTB}_4$  through exosomes does not necessarily translate into higher recruitment ranges or higher directionality in steady fMLP gradients, it plays a pivotal role in decaying fMLP gradients. We show that by their time-delayed release of  $\text{LTB}_4$ , exosomes can better preserve  $\text{LTB}_4$  after fMLP stimulus decreases. The model predicts that under such conditions exosomes maintain persistence of cell migration by conserving gradients over time periods that are determined by the rate at which exosomes are depleted of  $\text{LTB}_4$ . This could explain why the recruitment of neutrophils to sites of infection occurs in multiple phases, even after the initial recruitment signal dissipates (Ng et al., 2011). We also show that under high tissue concentrations of primary chemoattractant, for example, bolus production of  $\text{LTB}_4$  in response to *Mycobacterium* infection (El-Ahmady et al., 1997), packaging of  $\text{LTB}_4$  in exosomes could prevent receptor saturation and maintain cell motion. Conversely, exosomes may help sequester  $\text{LTB}_4$  in situations where it is rapidly removed from the tissue space, for example, near a draining lymphatic vessel. The use of vesicles as a secretion mechanism is not unique to  $\text{LTB}_4$  and is important for the formation of morphogen gradients during *Drosophila* embryogenesis (Entchev and González-Gaitán, 2002) and the diffusion of lipid-adducted molecules such as Wnt (The and Perrimon, 2000).

Neutrophil gradient sensing is best predicted by differences in chemoattractant receptor occupancy or DFRO (Tranquillo et al., 1988). DFRO has commonly been treated as proportional to cell flux (Tranquillo et al., 1988) or chemotactic index (Herzmark et al., 2007). The problem with this assumed proportionality is that, for a high-enough DFRO, a chemotactic index of greater than 1 would be predicted, which is not possible. To overcome this problem, we previously developed a model of cell migration in which DFRO determined the probability distributions of cell orientations (Szatmary and Nossal, 2017). From these probability distributions, we calculated fluxes of cells in chemotaxis assays. To study signal relay, rather than calculating fluxes of ensembles of cells, we assigned orientations to cells based on their individual probability distributions. Notably, our model also differs from early models of group migration by accounting for individual cells rather than cell densities (e.g., Keller and Segel, 1971; Tranquillo et al., 1988). Models of the mechanisms underlying transduction of gradient signals have clarified how gradient sensing works in individual cells (Irimia et al., 2009; Van Haastert, 2010; Xiong et al., 2010). Nevertheless, at this point, determining cell orientations from DFRO is the most effective way to realistically model gradient sensing in the context of migration of a large number of cells.

In our model, neutrophil sensitivity to formyl peptides,  $S_F$ , is calibrated to a systematically collected data set (Zigmond, 1977). Neutrophil sensitivity to LTB<sub>4</sub>,  $S_L$ , has not been measured as reliably, so we assume  $S_L = S_F$ . Neutrophils preferentially respond to formyl peptides relative to LTB<sub>4</sub> (Heit et al., 2002). We expressed this in our model by using Eq. 12 and selecting a value for  $F_{xt}$  that allowed the model to recapitulate this observation. Despite uncertainty about some properties of neutrophil response, our model recapitulates the in vivo observations of Lämmermann et al. (2013) that LTB<sub>4</sub>-mediated signal relay increases recruitment range and that LTB<sub>4</sub> is involved in prolonging recruitment.

Our model accounts for LTB<sub>4</sub> diffusion in one dimension (1D). This is appropriate because, in the problems we consider here, the fMLP concentration varies only in 1D, and LTB<sub>4</sub> secretion is driven by the fMLP concentration. Also, LTB<sub>4</sub> is secreted by a large number of evenly distributed cells. Therefore, we expect the LTB<sub>4</sub> concentration to vary primarily in one direction. At the level of a single cell, the secreted LTB<sub>4</sub> spreads out in 2D, so the resulting gradient would differ from what a 1D model would predict. However, in the present situation, 2D gradients arising from many secreting cells coalesce into a single gradient that is effectively 1D for the cells that are guided by it. Therefore, the effect of this approximation is negligible. Thus, accounting for only 1D diffusion is sufficient for the particular problems analyzed in this work. Of course, accounting for diffusion in 1D is not adequate for modeling every signal relay process. For example, accounting for diffusion in at least two dimensions is important for modeling the streaming of *Dictyostelium* cells (Guyen et al., 2013).

In the absence of detailed data, we assumed that neutrophil secretion rates depend only on the current concentration of fMLP and that exosomes secrete LTB<sub>4</sub> at exponentially decaying rates. Because LTB<sub>4</sub> is a sparingly soluble lipid, we also assumed that an LTB<sub>4</sub> molecule undergoes pure diffusion, followed by irreversible removal from solution with first-order kinetics. However, the secretion, motion, or removal of LTB<sub>4</sub> may be more complex than this, and many of the parameters required to build this model are not well known. Subsequent modeling efforts that explore the effects of varying these parameters can indicate how signal relay depends on changes in these parameters, such as may occur in disease states. While accounting for these features is not necessary to model gross aspects of signal relay, including them in future modeling efforts may reveal important aspects of this phenomenon.

Measuring the effects of LTB<sub>4</sub> on recruitment range is difficult with most existing assays. We suggest that relay works by neutrophils generating an LTB<sub>4</sub> profile that extends beyond where the primary fMLP gradient is steep enough to be sensed. Study of this aspect of relay in vitro requires assays in which slopes are shallower farther from the primary gradient source. The bridge (Zigmond, 1977), Dunn (Zicha et al., 1991), Taxiscan (Kanegasaki et al., 2003), and filter (Boydén, 1962) assays are not suitable for measuring recruitment range because they generate gradients of uniform slope. Finally, although microfluidic mixers can be used to generate and sustain nonlinear gradients (e.g., in Wang et al., 2004), they do so by continuously flowing the medium through the chamber, which would disrupt secondary gradients. It is, therefore, difficult to precisely design an in vitro measurement of neutrophil signal relay and chemotaxis assays such as the under-agarose assay are, at best, approximations. While in vivo methods are currently the best way to set up conditions in which changes in recruitment range can be observed, in vitro methods are better suited for making measurements in well-defined environments. Mathematical models can unite these approaches.

The present work primarily models signal relay in neutrophils but can be easily applied to other systems where a secondary chemoat-

tractant plays an important role in group migration. Given the widespread use of exosomes as means to distribute morphogens and other gradient forming agents, we envision that exosomes may be important in shaping gradients in other systems as well.

## MATERIALS AND METHODS

### Cell orientation

We have previously described our methods for modeling gradient sensing and chemoattractant transport (Szatmary and Nossal, 2017) and offer a brief overview here. We treat the cells as having orientations that fall on a von Mises–Fisher distribution, which is a kind of bell curve. This is used to represent the observation that stronger gradient signals (i.e., higher DFRO) cause cell orientations to be more biased toward the gradient direction. The von Mises–Fisher distribution is given by

$$f(\theta; \kappa) = \frac{\exp(\kappa \cos(\theta))}{2\pi I_0(\kappa)} \quad (13)$$

where  $\theta$  is the angle defined with respect to the direction of the chemoattractant gradient and  $I_0(\cdot)$  is the modified Bessel function of order 0;  $f(\theta; \kappa)$  is used here for representing 2D cell migration. The  $\kappa$  parameter represents the “bias” in the cell orientation distribution; a more-biased distribution has a greater number of cells oriented more directly up the gradient. We assume that bias is proportional to the difference in fractional receptor occupancy, that is,

$$\kappa = S \cdot \text{DFRO} \quad (14)$$

where  $S$  is the “sensitivity.” This  $S$  parameter depends on the cell type and identity of the chemoattractant. We previously estimated the sensitivity of neutrophils to formyl peptides (Szatmary and Nossal, 2017) by comparing Zigmond’s observations of cell orientation distributions with gradient conditions (Zigmond, 1977). Similar measurements have not been made for neutrophil response to LTB<sub>4</sub>, so, for simplicity, we assume that a neutrophil would be equally responsive in an LTB<sub>4</sub> gradient as in an equivalent fMLP gradient. For each cell at each timestep, we used Eq. 12 to calculate  $\kappa$ . The Scipy vonmises function then generated a random angle drawn from the von Mises distribution with this particular  $\kappa$ , and the cell then traveled at this angle during the next time step.

### Determination of chemoattractant gradients

To determine the distributions of LTB<sub>4</sub> and exosomes, we solved Eqs. 5 and 7 using numerical methods. Chemoattractant concentration profiles were calculated by solving the diffusion equation with the finite-difference method using Adams predictor-corrector methods for time stepping; this was implemented with the odeint function from SciPy (Oliphant, 2007), which is an interface for the LSODE solver from ODEPACK (Hindmarsh, 1983). We previously validated our numerical methods (Szatmary et al., 2014) by comparison with the findings of Lauffenburger and Zigmond (1981).

### Cell lines and constructs

PLB985 cells expressing mCherry-5LO and CD63-GFP as well as co-expressing both CD63-GFP and mCherry-5LO were created using a retroviral approach as described previously (Majumdar et al., 2016).

### Chemotaxis assay and image acquisition

HL-60 cells were differentiated at a density of  $4.5 \times 10^5$  cells/ml for 6 d in culture medium containing 1.3% dimethyl sulfoxide (DMSO), and the status of differentiation was monitored by CD11b staining. Differentiated cells were plated on chambered cover slides coated

with fibronectin (10  $\mu\text{g/ml}$ ), and a chemotactic gradient was generated using an Eppendorf microinjector with Femtotips (Eppendorf, Germany) loaded with 1  $\mu\text{M}$  fMLP. For steady-state cell migration, the under-agarose assay, described elsewhere, was performed 2 h post addition of fMLP (Majumdar *et al.*, 2016). Images of exosome release by migrating cells were acquired using Instant Structured Illumination Microscope (iSIM) super-resolution microscopy as described previously (Curd *et al.*, 2015).

## ACKNOWLEDGMENTS

We thank the members of the Nossal and Parent laboratories for helpful discussions. We also thank Hari Shroff, National Institute of Biomedical Imaging and Bioengineering, National Institutes of Health, for his help in iSIM microscopy. This study was supported by the Intramural Research Programs of the Eunice Kennedy Shriver National Institute of Child Health and Human Development and the Center for Cancer Research, National Cancer Institute, National Institutes of Health.

## REFERENCES

- Afonso PV, Janka-Junttila M., Lee YJ, McCann CP, Oliver CM, Aamer KA, Losert W, Cicerone MT, Parent CA (2012). LTB4 is a signal-relay molecule during neutrophil chemotaxis. *Dev Cell* 22, 1079–1091.
- Berg HC, Purcell EM (1977). Physics of chemoreception. *Biophys J* 20, 193–219.
- Boyden S (1962). The chemotactic effect of mixtures of antibody and antigen on polymorphonuclear leucocytes. *J Exp Med* 115, 453–466.
- Curd A, Cleasby A, Makowska K, York A, Shroff H, Peckham M (2015). Construction of an instant structured illumination microscope. *Methods* 88, 37–47.
- Dahlgren C, Magnusson KE, Sundqvist T (1984). Concentration gradients in the under-agarose chemotaxis assay system with attractant surface adsorption. *J Immunol Methods* 75, 23–29.
- Dorner BG, Dorner MB, Zhou X, Opitz C, Mora A, Guttler S, Hutloff A, Mages HW, Ranke K, Schaefer M, *et al.* (2009). Selective expression of the chemokine receptor XCR1 on cross-presenting dendritic cells determines cooperation with CD8+ T cells. *Immunity* 31, 823–833.
- El-Ahmady O, Mansour M, Zoer H, Mansour O (1997). Elevated concentrations of interleukins and leukotriene in response to mycobacterium tuberculosis infection. *Ann Clin Biochem* 34, 160–164.
- Entchev EV, González-Gaitán MA (2002). Morphogen gradient formation and vesicular trafficking. *Traffic* 3, 98–109.
- Foxman EF, Campbell JJ, Butcher EC (1997). Multistep navigation and the combinatorial control of leukocyte chemotaxis. *J Cell Biol* 139, 1349–1360.
- Garcia GL, Parent CA (2008). Signal relay during chemotaxis. *J Microsc* 231, 529–534.
- Gouwy M, De Buck M, Portner N, Opdenakker G, Proost P, Struyf S, Van Damme J (2015). Serum amyloid A chemoattracts immature dendritic cells and indirectly provokes monocyte chemotaxis by induction of cooperating CC and CXC chemokines. *Eur J Immunol* 45, 101–112.
- Guvan C, Rericha E, Ott E, Losert W (2013). Modeling and measuring signal relay in noisy directed migration of cell groups. *PLoS Comput Biol* 9, e1003041.
- Haessler U, Pisano M, Wu M, Swartz MA (2011). Dendritic cell chemotaxis in 3D under defined chemokine gradients reveals differential response to ligands CCL21 and CCL19. *Proc Natl Acad Sci USA* 108, 5614–5619.
- Heit B, Tavener S, Raharjo E, Kubers P (2002). An intracellular signaling hierarchy determines direction of migration in opposing chemotactic gradients. *J Cell Biol* 159, 91–102.
- Herzmark P, Campbell K, Wang F, Wong K, El-Samad H, Groisman A, Bourne HR (2007). Bound attractant at the leading vs. the trailing edge determines chemotactic prowess. *Proc Natl Acad Sci USA* 104, 13349–13354.
- Hindmarsh AC (1983). ODEPACK, A Systematized Collection of ODE Solvers, IMACS Transactions on Scientific Computation, Vol. 1, ed. RS Stepleman *et al.*, Amsterdam: North-Holland, 55–64.
- Irimia D, Balazsi G, Agrawal N, Toner M (2009). Adaptive-control model for neutrophil orientation in the direction of chemical gradients. *Biophys J* 96, 3897–3916.
- Jin T, Xu X, Hereld D (2008). Chemotaxis, chemokine receptors and human disease. *Cytokine* 44, 1–8.
- Kanegasaki S, Nomura Y, Nitta N, Akiyama S, Tamatani T, Goshoh Y, Yoshida T, Sato T, Kikuchi Y (2003). A novel optical assay system for the quantitative measurement of chemotaxis. *J Immunol Methods* 282, 1–11.
- Keller EF, Segel LA (1971). Model for chemotaxis. *J Theor Biol* 30, 225–234.
- Kelner GS, Kennedy J, Bacon KB, Kleyensteuber S, Largaespada DA, Jenkins NA, Copeland NG, Bazan JF, Moore KW, Schall TJ, *et al.* (1994). Lymphotactin: a cytokine that represents a new class of chemokine. *Science* 266, 1395–1399.
- Kim BJ, Hannanta-Anan P, Chau M, Kim YS, Swartz MA, Wu MM (2013). Cooperative roles of SDF-1 alpha and EGF gradients on tumor cell migration revealed by a robust 3D microfluidic model. *PLoS One* 8, e68422.
- Lämmermann T, Afonso PV, Angermann BR, Wang JM, Kastenmüller W, Parent CA, Germain RN (2013). Neutrophil swarms require LTB4 and integrins at sites of cell death in vivo. *Nature* 498, 371–375.
- Land WG (2015). The role of damage-associated molecular patterns in human diseases: Part I. Promoting inflammation and immunity. *Sultan Qaboos Univ Med J* 15, e9–e21.
- Lauffenburger DA, Zigmond SH (1981). Chemotactic factor concentration gradients in chemotaxis assay systems. *J Immunol Methods* 40, 45–60.
- Majumdar R, Sixt M, Parent CA (2014). New paradigms in the establishment and maintenance of gradients during directed cell migration. *Curr Opin Cell Biol* 30, 33–40.
- Majumdar R, Tavakoli Tameh A, Parent CA (2016). Exosomes mediate LTB4 release during neutrophil chemotaxis. *PLoS Biol* 14, e1002336.
- Ng LG, Qin JS, Roediger B, Wang Y, Jain R, Cavanagh LL, Smith AL, Jones CA, de Veer M, Grimbaldston MA, *et al.* (2011). Visualizing the neutrophil response to sterile tissue injury in mouse dermis reveals a three-phase cascade of events. *J Invest Dermatol* 131, 2058–2068.
- Oates AC, Gorfinkel N, Gonzalez-Gaitan M, Heisenberg C-P (2009). Quantitative approaches in developmental biology. *Nat Rev Genet* 10, 517–530.
- Oliphant TE (2007). Python for scientific computing. *Comput Sci Eng* 9, 10–20.
- Peters-Golden M, Henderson WRJ (2007). Leukotrienes. *N Engl J Med* 357, 1841–1854.
- Szatmary AC, Nossal R (2017). Determining whether observed eukaryotic cell migration indicates chemotactic responsiveness or random chemokinetic motion. *J Theor Biol* 425, 103–112.
- Szatmary AC, Stuelten CH, Nossal R (2014). Improving the design of the agarose spot assay for eukaryotic cell chemotaxis. *RSC Adv* 4, 57343–57349.
- The I, Perrimon N (2000). Morphogen diffusion: the case of the Wingless protein. *Nat Cell Biol* 2, E79–E82.
- Tranquillo RT, Zigmond SH, Lauffenburger DA (1988). Measurement of the chemotaxis coefficient for human neutrophils in the under-agarose migration assay. *Cell Motil Cytoskeleton* 11, 1–15.
- Uden AM, Hafstrom I, Palmblad J (1986). Relation to chemotactic factor gradients to neutrophil migration and orientation under agarose. *J Leukoc Biol* 39, 27–35.
- Van Haastert PJ (2010). A stochastic model for chemotaxis based on the ordered extension of pseudopods. *Biophys J* 99, 3345–3354.
- Vicker MG, Lackie JM, Schill W (1986). Neutrophil leucocyte chemotaxis is not induced by a spatial gradient of chemoattractant. *J Cell Sci* 84, 263–280.
- Wang SJ, Saadi W, Lin F, Minh-Canh Nguyen C, Li Jeon N (2004). Differential effects of EGF gradient profiles on MDA-MB-231 breast cancer cell chemotaxis. *Exp Cell Res* 300, 180–189.
- Wang Y, Irvine DJ (2013). Convolution of chemoattractant secretion rate, source density, and receptor desensitization direct diverse migration patterns in leukocytes. *Integr Biol (Camb)* 5, 481–494.
- Wartlick O, Kicheva A, Gonzalez-Gaitan M (2009). Morphogen gradient formation. *Cold Spring Harb Perspect Biol* 1, a001255.
- Xiong Y, Huang CH, Iglesias PA, Devreotes PN (2010). Cells navigate with a local-excitation, global-inhibition-biased excitable network. *Proc Natl Acad Sci USA* 107, 17079–17086.
- Yoon YJ, Gho YS (2014). Extracellular vesicles as emerging intercellular communicasomes. *BMB Rep* 47, 531–539.
- Zicha D, Dunn GA, Brown AF (1991). A new direct-viewing chemotaxis chamber. *J Cell Sci* 99(Pt 4), 769–775.
- Zigmond SH (1977). Ability of polymorphonuclear leukocytes to orient in gradients of chemotactic factors. *J Cell Biol* 75, 606–616.